Bilayer Properties of Totally Synthetic C16:0-Lactosyl-Ceramide

Kumkum Saxena,* Peter Zimmermann,[†] Richard R. Schmidt,[†] and G. Graham Shipley*
*Departments of Biophysics and Biochemistry, Center for Advanced Biomedical Research, Boston University School of Medicine, Boston, Massachusetts 02118 USA, and [†]Fakultat Chemie, Universitat Konstanz, D-78457 Konstanz, Germany

ABSTRACT   Differential scanning calorimetry (DSC) and x-ray diffraction have been used to study the structural and thermal properties of totally synthetic D-erythro-N-palmitoyl-lactosyl-C$_{18}$-sphingosine (C16:0-LacCer). Over the temperature range 0–90°C, fully hydrated C16:0-LacCer shows complex thermal transitions characteristic of polymorphic behavior of exclusively bilayer phases. On heating at 5°C/min, hydrated C16:0-LacCer undergoes a complex two-peak endothermic transition with maxima at 69°C and 74°C and a total enthalpy of 14.6 kcal/mol C16:0-LacCer. At a slower heating rate (1.5°C/min), two endothermic transitions are observed at 66°C and 78°C. After cooling to 0°C, the subsequent heating run shows three overlapping endothermic transitions at 66°C, 69°C, and 71.5°C, followed by a chain-melting endothermic transition at 78°C. Two thermal protocols were used to completely convert C16:0-LacCer to its stable, high melting temperature (78°C) form. As revealed by x-ray diffraction, over the temperature range 20–78°C this stable phase exhibits a bilayer structure, periodicity $d \approx 65$ Å with an ordered chain packing mode. At the phase transition (78°C) chain melting occurs, and C16:0-LacCer converts to a liquid crystalline bilayer (L$_\alpha$) phase of reduced periodicity $d \approx 59$ Å. On cooling from the L$_\alpha$ phase, C16:0-LacCer converts to metastable bilayer phases undergoing transitions at 66–72°C. These studies allow comparisons to be made with the behavior of the corresponding C16:0-Cer (Shah et al., 1995. J. Lipid Res. 36:1936–1944) and C16:0-GluCer and C16:0-GalCer (Saxena et al., 1999. J. Lipid Res. 40:839–849). Our systematic studies are aimed at understanding the role of oligosaccharide complexity in regulating glycosphingolipid structure and properties.

INTRODUCTION

Phospholipids, glycosphingolipids (GSLs), and cholesterol are the major constituents of the lipid bilayer compartment of cell membranes. This lipid bilayer provides the matrix in which functional membrane proteins (enzymes, receptors, channels, etc.) are inserted. While all of these lipids appear to contribute to the structural stability of the bilayer, it has become increasingly obvious that many of the lipid components play additional functional roles. For example, phospholipids are involved in cell signaling processes (Exton, 1994; Nishizuka, 1992; Berridge, 1993; Hannun, 1994), serving as substrates for lipolytic enzymes (phospholipases) to release second messengers (arachidonic acid/prostaglandins, inositol phosphates, diglycerides, ceramides, etc.). In contrast, GSLs are thought to be involved in cell-cell communication (Hakomori and Igarashi, 1995) and can act as cell surface receptors for hormones, bacterial toxins, and viruses (Harouse et al., 1991; van den Berg et al., 1992; Fishman et al., 1993).

GSLs are complex lipids with a lipophilic ceramide (N-acyl sphingosine) component linked to a hydrophilic oligosaccharide. Our research has focused on describing the structure and properties of different GSLs. In particular, we have focused on 1) natural GSLs with heterogeneous fatty acyl chains (Curatolo et al., 1977; Ruocco and Shipley, 1986), 2) partially synthetic GSL with controlled fatty acid composition but some variability in the sphingosine moiety (Ruocco et al., 1981; Reed and Shipley, 1987, 1989; Haas and Shipley, 1995), and, most recently, 3) totally synthetic GSLs, pure with respect to stereochemistry and chain and sphingosine composition (Shah et al., 1995; Saxena et al., 1999). Our goal is to build up a picture of the contributions of acyl chain structure (chain length, unsaturation, hydroxylation), sphingosine structure (chain length, unsaturation, hydroxylation), and, most importantly, oligosaccharide complexity to GSL structure, hydration, and properties. For the latter, we have investigated totally synthetic ceramides, D-erythro-N-palmitoyl-C$_{18}$-sphingosine (C16:0-Cer), lacking a sugar component (Shah et al., 1995), and monoglycosylceramides, D-erythro-N-palmitoyl-galactosyl-C$_{18}$-sphingosine (C16:0-GalCer) and D-erythro-N-palmitoyl-glucosyl-C$_{18}$-sphingosine (C16:0-GluCer) (Saxena et al., 1999). In this paper we report on the behavior of the diglycosylceramide D-erythro-N-palmitoyl-lactosyl-C$_{18}$-sphingosine (C16:0-LacCer) and compare it with that of the single sugar compounds, C16:0-GalCer and C16:0-GluCer. In all cases we are studying GSLs that are pure with respect to their sphingosine stereochemistry (D-erythro), their fatty acid composition (C16:0; palmitoyl), and their sphingosine structure (C18:1, Δ4–5, trans), in this case N-palmitoyl-lactosyl-D-erythro-sphingosine containing the disaccharide β-D-galactosyl-(1→4)-β-D-glucose (Glu-Gal). Future studies will focus on the recently synthesized ganglioside C16:0-G$_{M3}$ (R. I. Duclos, Jr. and G. G. Shipley, unpublished results) containing the trisaccharide Glu-Gal-N-acetyl neuraminic acid (Glu-Gal-NANA) and eventually the penta-

saccharide-containing ganglioside C16:0-G$_{M1}$. This approach should certainly provide an improved picture of the role of the sugar moiety in regulating GSL phase behavior and perhaps the functional role of GSLs in membranes. For example, we are particularly interested in the function of ganglioside G$_{M1}$ as a receptor for cholera toxin (Reed and Shipley, 1996; Reed et al., 1987; Zhang et al., 1995a,b).

MATERIALS AND METHODS

Synthesis

Totally synthetic *N*-palmitoyl-lactosyl-D-erythro-sphingosine was synthesized starting from D-galactose, as described previously by Schmidt and colleagues (Schmidt and Zimmermann, 1986; Zimmermann et al., 1988).

Differential scanning calorimetry

Aliquots of C16:0-LacCer containing 1–4 mg of lipid, in chloroform-methanol (2:1 v/v), were transferred directly into preweighed stainless steel differential scanning calorimetry (DSC) pans, dried under N$_2$ and, subsequently, in vacuo overnight. The pans containing dried C16:0-LacCer were reweighed, and double-distilled water was added to the pans with a microsyringe to obtain the required hydration. The pans were then hermetically sealed. Heating and cooling scans over the temperature range 0–90°C were performed on a Perkin-Elmer (Norwalk, CT) DSC-2 or DSC-7 calorimeter. Heating and cooling rates ranged from 0.1 to 40°C/min. Peak maxima (or minima) were taken as the transition temperature. Transition enthalpies were determined from the area under the transition peak by comparison with those for a known standard (gallium). Baselines in the region of the transition were approximated by extrapolating the pretransition baseline to the posttransition baseline. DSC measurements of dilute dispersions (~2 mg C16:0-LacCer/ml) were also made with a Microcal (MC-2) scanning calorimeter (Microcal, Springfield, MA) at a heating rate of 1.5°C/min.

X-ray diffraction

Hydrated samples for x-ray diffraction were prepared by weighing anhydrous C16:0-LacCer into thin-walled glass capillary tubes (internal diameter, 1 mm) followed by gravimetric addition of distilled, deionized water. Samples were covered with parafilm, centrifuged at room temperature for ~2 min, reweighed, and then flame-sealed. Homogeneous dispersions were obtained through a repeated cycle of centrifugation-sample inversion-centrifugation at 68°C. Based on the DSC studies (see below), sample equilibration is achieved with incubation at this temperature. Nickel-filtered CuK$_\alpha$ X-radiation from an Elliot GX-6 rotating anode generator (Elliot Automation, Borehamwood, U.K.) was focused by either a toroidal mirror or double-mirror optical system into a point source. X-ray diffraction patterns were recorded with photographic film.

RESULTS

Differential scanning calorimetry

Representative calorimetric scans of equilibrated fully hydrated (70 wt % water) C16:0-LacCer are shown in Fig. 1. On heating at 5°C/min, a complex two-peak endotherm with maxima at 69°C and 74°C (Fig. 1 *a*) is observed with a total enthalpy $\Delta H = 14.6$ kcal/mol LacCer. On cooling from 90°C at 5°C/min, a single relatively sharp exotherm at 53°C
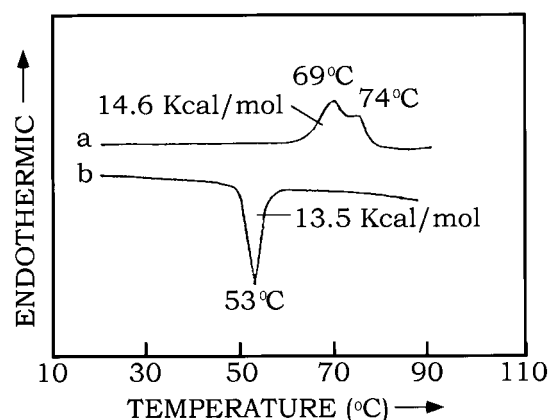

FIGURE 1 Differential scanning calorimetry of fully hydrated (70 wt % water) C16:0-LacCer using the Perkin-Elmer DSC-7 calorimeter. (*a*) Heating scan, 5°C/min. (*b*) Cooling scan, 5°C/min.

(enthalpy $\Delta H = 13.5$ kcal/mol) is observed. Successive heating and cooling scans at 5°C/min showed essentially the same behavior. The pronounced hysteresis observed clearly indicates a slow equilibration process on cooling from the melted-chain state.

To further probe the polymorphic phase behavior of hydrated C16:0-LacCer, heating runs were recorded at a slower heating rate (1.5°C/min) in the high-sensitivity Microcal calorimeter. Fig. 2 *a* shows the first heating scan of an unequilibrated sample of hydrated C16:0-LacCer (2 mg/ml) recorded at 1.5°C/min. Two endothermic transitions are observed at 66°C and 78°C, behavior similar but not identical to that shown in Fig. 1. However, at this slower heating rate there is also evidence of an exothermic transition centered at ~68°C, i.e., between the two endothermic transitions. After cooling to 0°C, the subsequent heating run (Fig. 2 *b*) shows somewhat different behavior, with three overlapping endothermic transitions at 66°C, 69°C, and 71.5°C, followed by a small endothermic transition at 78°C. The highest transition observed (at 78°C), although of varying
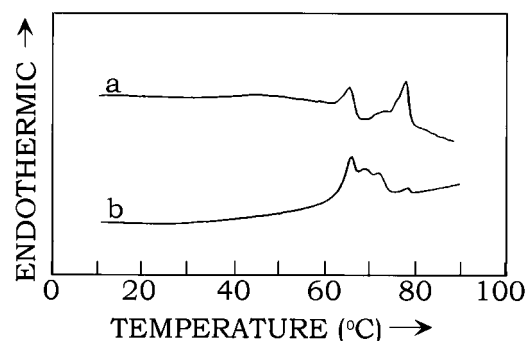

FIGURE 2 Differential scanning calorimetry of fully hydrated (2 mg/ml) C16:0-LacCer, recorded with a Microcal MC-2 calorimeter. (*a*) Initial heating scan (0 to 90°C) at 1.5°C/min. (*b*) Next heating scan at 1.5°C/min after cooling to 0°C.

enthalpy (see Fig. 2), presumably represents the conversion of the most stable form of hydrated C16:0-LacCer to the melted-chain phase. Corresponding transitions of hydrated C16:0-GalCer and C16:0-GlcCer occur at 85°C and 87°C, respectively. Two additional protocols were used to completely convert C16:0-LacCer to its most stable form.

First, if the initial heating run of C16:0-LacCer is terminated at 68°C (corresponding to the exothermic transition; see Figs. 2 *a* and 3 *a*), followed by cooling to 0°C, the subsequent heating run shows none of the transitions in the temperature range 66–72°C (compare Figs. 3 *b* and 2 *b*); instead, only the high temperature transition at 78°C with significantly increased enthalpy is observed (compare Figs. 3 *b* and 2 *b*). After cooling to 0°C, the next heating scan (Fig. 3 *c*) showed two transitions in the temperature range 66–72°C, followed by the 78°C transition with significantly reduced enthalpy. Further cooling and heating cycles led to the reappearance of the original three overlapping transitions between 66°C and 72°C and further loss of enthalpy associated with the 78°C transition (Figs. 3, *d–f*). Further heating/cooling cycles exhibit essentially identical heating scans, C16:0-LacCer appears to be "equilibrated," and the 78°C transition is not observed. The most stable phase of hydrated C16:0-LacCer can also be produced by incubating the sample at 68.5°C, immediately after the initial transition

at 66°C (see Fig. 3 *g*) for 2 h or longer. After cooling, the next heating scan (Fig. 3 *h*) shows only the high-temperature, high-enthalpy transition at 78°C (compare Fig. 3, *h* and *b*). Further cooling/heating cycles result in heating scans similar to those shown in Fig. 3, *c–f* (data not shown).

X-ray diffraction

Structural information on the phases of hydrated C16:0-LacCer was obtained by recording x-ray diffraction patterns at different temperatures (see *lettered arrows* in Fig. 3). After equilibration at 68°C and cooling to 20°C, the x-ray diffraction pattern shown in Fig. 4 *A* is obtained. Based on three low-angle lamellar reflections, the bilayer periodicity of this phase is 65.5 Å. The wide-angle region shows two sharp reflections at $1/4.36$ Å^{-1} and $1/4.11$ Å^{-1}, as well as other, weaker reflections. After heating to 68°C, the x-ray diffraction pattern recorded at this temperature (Fig. 4 *B*) is essentially identical to that observed at 20°C (compare Fig. 4, *A* and *B*). The bilayer periodicity is decreased slightly to 64.5 Å, and there are small shifts in the wide-angle reflections ($1/4.43$ Å^{-1} and $1/4.17$ Å^{-1}). Continued heating to 75°C results in a diffraction pattern identical to that shown in Fig. 4 *B* (data not shown). Above the 78°C transition, at 85°C, the diffraction pattern shown in Fig. 4 *C* is observed. Three lamellar, low-angle reflections index to a bilayer periodicity of 59.4 Å, and the diffuse wide-angle reflection at $1/4.6$ Å^{-1} is indicative of hydrocarbon chain melting (Fig. 4 *C*). After the sample is cooled from 85°C to 20°C, the x-ray diffraction pattern shown in Fig. 4 *D* is observed. This diffraction pattern differs from that originally observed at 0°C (compare Fig. 4, *C* and *A*). Three lamellar reflections corresponding to a bilayer periodicity $d = 52.5$ Å are observed; the wide-angle region is characterized by two reflections at $1/4.39$ Å^{-1} and $1/3.89$ Å^{-1}. Heating the sample to 68°C results in a complex x-ray diffraction pattern, as shown in Fig. 4 *E*. Two sets of lamellar low-angle reflections are observed that index according to bilayer periodicities of 65.5 Å and 58.9 Å. The wide-angle region is characterized by a strong reflection at $1/4.26$ Å^{-1} and two other reflections at $1/4.78$ Å^{-1} and $1/4.11$ Å^{-1}. Clearly two coexisting bilayer phases are present at 68°C as a result of this thermal protocol.

DISCUSSION

Our goal here is to summarize the thermotropic and structural behavior of C16:0-LacCer and to make comparisons with the behavior of other synthetic sphingolipids. Of particular interest is the effect of increasing the size of the oligosaccharide moiety attached to C16:0-ceramide on these properties. Only through the development of de novo methods for the synthesis of chemically and stereochemically pure sphingosines, ceramides, and glycosphingolipids can
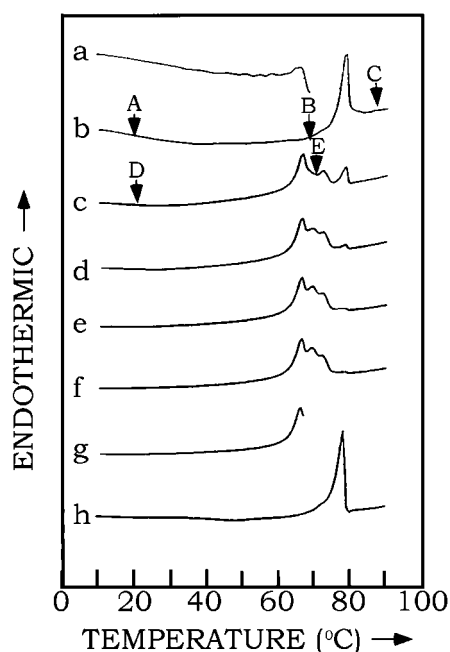
FIGURE 3 Differential scanning calorimetry of fully hydrated (2 mg/ml) C16:0-LacCer, recorded with a Microcal MC-2 calorimeter. Heating scans were at 1.5°C/min. (*a*) Initial heating scan, 10–68°C. (*b-f*) Subsequent heating scans. The sample was cooled to 0°C and heating scans at 10–90°C were recorded immediately. (*g*) The sample was heated to 68.5°C and incubated at this temperature for 2 h. (*h*) Heating scan, 10–90°C, immediately after cooling to 0°C. Lettered arrows indicate temperatures at which x-ray diffraction experiments were performed (see Fig. 4).
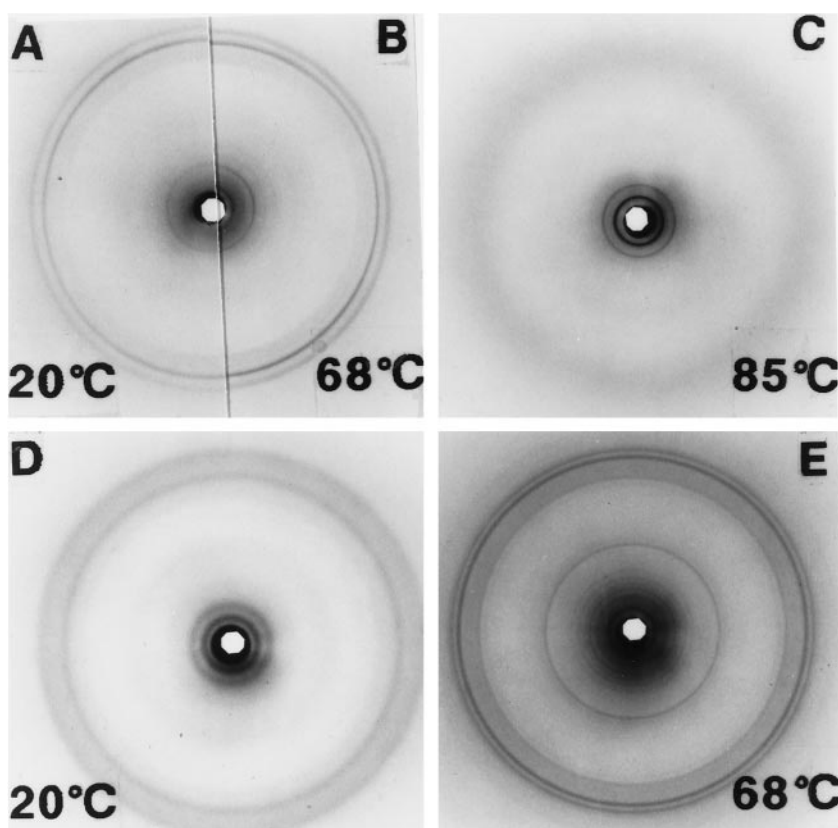
FIGURE 4 X-ray diffraction patterns of fully hydrated (70 wt % water) C16:0-LacCer at different temperatures. (*A*) Initial exposure at 20°C; sample temperature had not exceeded 68°C. (*B*) 68°C. (*C*) 85°C. (*D*) 20°C (after cooling from 85°C). (*E*) 68°C (after cooling from 85°C to 20°C and reheating to 68°C).

the contributions of heterogeneities in acyl chain composition (length/unsaturation), sphingosine chemistry, and stereochemistry to GSL behavior be eliminated.

Thermotropic behavior

At a heating rate of 5°C/min, hydrated C16:0-LacCer shows two overlapping endotherms at 69°C and 74°C, whereas on cooling a single transition at 53°C is observed (Fig. 1); repeated cycles of heating and cooling at 5°C/min show essentially the same behavior. The multiple transitions observed on heating are indicative of lipid polymorphic behavior, whereas the hysteresis behavior observed on cooling is indicative of the slow conversion from the melted chain L_α bilayer phase to the more ordered gel or crystalline phase. This hysteresis behavior has been observed for synthetic C16:0-ceramides (Shah et al., 1995) and different natural, partially synthetic, and totally synthetic cerebrosides (Ruocco et al., 1981; Curatolo, 1982; Reed and Shipley, 1987, 1989; Haas and Shipley, 1995; Saxena et al., 1999). Thus this behavior appears to be particularly prevalent for GSLs and is less consistently observed for phospholipids, for example. At a slower heating rate (1.5°C/min), the first heating scan (Fig. 2 *a*) of C16:0-LacCer shows different behavior presumably due to both 1) the heating of an initially unequilibrated C16:0-LacCer/water sample and 2) the slow heating rate. The initial endothermic

transition at ~66°C is followed by an exotherm at ~68°C, and then a major endothermic transition is observed at 78°C. Presumably the 78°C transition represents conversion of an exothermically produced stable form of C16:0-LacCer undergoing hydrocarbon chain melting to a liquid crystalline form (see below).

However, after cooling, the next heating scan exhibits three overlapping transitions with maxima at 66°C, 69°C, and 72°C (Fig. 2 *b*), and only a minor transition is observed at 78°C. The three low-temperature transitions at 66°C, 69°C, and 72°C probably represent interconversion of various metastable forms. From this point, repeated cooling/heating cycles show some variability, most notably the progressive decrease in the enthalpy associated with the 78°C transition (see, for example, Fig. 3, *c–e*). Two slightly different protocols were used to convert C16:0-LacCer to its most stable form, either during the initial heating scan (Fig. 3, *a* and *b*) or after cooling from the high-temperature, presumably chain-melted, form (Fig. 3, *g* and *h*). The former involved heating to the exothermic transition at ~68°C and cooling (Fig. 3 *a*), whereas the latter required incubation at 68°C followed by cooling (Fig. 3 *g*). Presumably both procedures lead to *complete* exothermic conversion to the stable, high melting temperature (78°C) form (Fig. 3, *b* and *h*).

Interestingly, hydrated C16:0-Cer, -GalCer, and -GluCer, and now -LacCer are all capable of exhibiting an exother-

FIGURE 5 Schematic representation of the temperature-dependent structural changes of fully hydrated C16:0-LacCer.
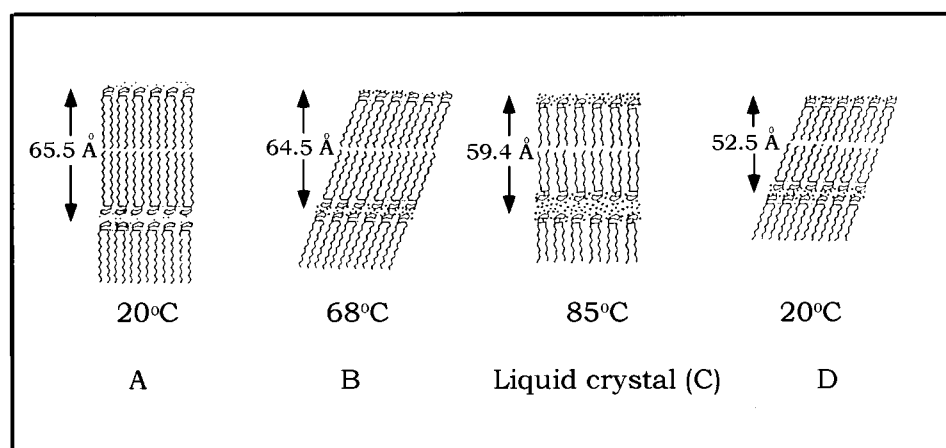
mic conversion from a metastable form to a stable, high melting temperature form. The stable form undergoes chain melting to a liquid crystalline phase; the temperature decreases in the sequence C16:0-Cer (90°C) > -GluCer (87°C) > -GalCer (85°C) > -LacCer (78°C). Thus the sequential addition of saccharide units to the parent C16:0 ceramide leads to a progressive decrease in the stability of the stable phase (or conversely, an increase in the stability of the melted-chain, liquid crystalline phase). The higher transition temperatures (78–90°C) exhibited by these sphingosine-based lipids compared to synthetic phospholipids (40–50°C) is thought to be due to both increased hydrogen bond capabilities in the sphingosine interfacial region and a highly ordered, "crystalline" chain packing mode. Interestingly, we now show that the addition of sugars actually results in a decrease in the stability of the stable phase. Thus sequential addition of sugar units may in fact present a lateral molecular packing problem due to incompatibilities between the packing requirements of the sugar headgroups and the underlying interfacial and chain packing modes.

Structural behavior

We have used x-ray diffraction to characterize the structures of some, but not all, of the phases exhibited by hydrated C16:0-LacCer (see Fig. 5). First, the stable phase that exists from 0–78°C exhibits a lamellar bilayer structure with a bilayer periodicity $d = 65.5$ Å (Fig. 4, A and B). The presence of several sharp reflections in the wide-angle region (the two strongest at 1/4.36 and 1/4.11 Å^{-1}) are indicative of an ordered ("crystalline") chain packing arrangement in this bilayer phase of C16:0-LacCer. This stable bilayer phase is present up to 78°C (for example, see Fig. 4 B), at which point the stable phase undergoes chain melting. While differences in the chain packing mode of the stable phases of C16:0-Cer, -GalCer, -GluCer, and -LacCer are evident from differences in the pattern of the strong

wide-angle reflections, we note that the bilayer periodicity of the stable phase increases with the addition of sugars; thus, C16:0-Cer ($d = 41.8$ Å) < -GluCer (53.9 Å) < -GalCer (55.2 Å) < -LacCer (65.5 Å). Thus, the addition of a single sugar (Glu or Gal) to C16:-Cer leads to an increase in periodicity of 12–13 Å; the second sugar results in a further 10–12-Å increment. These data suggest that the mono- and disaccharide units orient with their long axes parallel to the bilayer normal. However, it should be pointed out that both the thickness of the hydration layer and chain tilt contribute to the measured bilayer periodicity, and it is not clear at this stage whether these structural parameters are identical for the different C16:0-GSLs studied. Interestingly, the two strong, sharp, wide-angle reflections of C16:0-LacCer (at 1/4.4 Å^{-1} and 1/4.1 Å^{-1}) are identical to those of C16:0-GluCer but differ from those of C16:0-GalCer (1/4.7 Å^{-1} and 1/4.2 Å^{-1}). Again, this might indicate that the common ceramide-glucose moiety of GluCer and LacCer produces a similar molecular packing and bilayer organization for C16:0-GluCer and -LacCer.

At 78°C, the transition temperature of the stable phase of C16:0-LacCer, a chain melting transition occurs and a lamellar, liquid crystalline phase forms, as shown by the presence of the diffuse wide-angle reflection at 1/4.6 Å^{-1}. At 84°C, the bilayer periodicity of this L_α phase is 59.4 Å. C16:0-Cer shows only a single broad low-angle reflection at 29.9 Å, suggesting a nonbilayer melted chain phase (perhaps inverse micellar, inverse hexagonal). The addition of a single sugar, either glucose or galactose, clearly favors the formation of a classical L_α bilayer phase; the bilayer periodicities for C16:0-GluCer and -GalCer are 50.8 and 50.2 Å, respectively. Thus addition of the second sugar unit, galactose, of LacCer results in a 9-Å increment to the bilayer periodicity, again suggesting (but not proving; see qualifying statements above for the stable phase) an orientation of the galactose group parallel to the membrane normal.

On cooling from the L_α bilayer phase to 20°C, a different bilayer phase, presumably corresponding to the metastable phase undergoing the 66°C transition, is formed. Paradoxically, as this phase forms from the L_α phase, the bilayer thickness actually *decreases* from 59.4 to 52.5 Å. Furthermore, the bilayer periodicity of this metastable phase is significantly smaller (52.5 versus 65.5 Å) than that of the stable phase described above, and its wide-angle reflections are different (1/4.39 Å^{-1} and 1/3.89 Å^{-1}). Thus major structural rearrangements must occur as this metastable phase is formed from the L_α phase and as it converts to the stable phase. There are no obvious structural correlations with the metastable phases of C16:0-Cer, -GluCer, or -GalCer.

It is interesting to note that the structure of the melted-chain phase of the chemically related glycoglycerolipids appears to depend on the number of attached sugar units. For example, the monoglycosyl-glycerolipids favor the formation of the nonbilayer hexagonal phase, whereas addition of a second sugar promotes the formation of bilayer lamellar phases (for example, see original studies of plant galactolipids by Shipley et al., 1973). Systematic studies of synthetic glycoglycerolipids differing in sugar structure, fatty acid chain length, and chain unsaturation have been reported by Quinn, Hinz, and McElhaney and their colleagues (for example, Sen et al., 1981; Hinz et al., 1991; Sen et al., 1990; Mannock et al., 1994). These extensive studies have essentially confirmed and extended the concept of an important structure-determining role for the lipid-linked sugar moiety. Thus, in this context, the ability of hydrated C16:0-LacCer to form the bilayer L_α phase (as reported here) is predictable. Perhaps more puzzling is the inability of the monoglycosyl GalCer and GluCer to form nonbilayers (e.g., hexagonal type II) irrespective of the chain length (C16, C18, or C24; Ruocco et al., 1981; Reed and Shipley, 1987, 1989; Saxena et al., 1999) or chain *cis*-unsaturation (C16:1, C18:1, C18:2, or C18:3; Reed and Shipley, 1989; Haas and Shipley, 1995), at least up to 100°C. Presumably some structural characteristic contributed by the sphingosine moiety favors the formation of a stable bilayer phase. Eventually this structural constraint is overridden, inasmuch as it is known that more complex glycosphingolipids (e.g., gangliosides) do form nonbilayer (hexagonal I) and micellar structures (Curatolo et al., 1977).

In summary, C16:0-LacCer, like totally synthetic C16:0-GluCer and -GalCer, forms exclusively bilayer phases. Notably, the addition of one or two hexose moieties to C16:0-Cer leads to a stable L_α phase. Furthermore, the addition of a second hexose group to GlcCer does not result in the formation of nonbilayer structures after chain melting. Clearly, additional sugar units, including charged sugars (e.g., NANA), are required before hydrated nonbilayer (hexagonal, cubic, or micellar) phases are favored.

REFERENCES

Berridge, M. J. 1993. Inositol triphosphate and calcium signalling. *Nature.* 361:315–325.

Curatolo, W. 1982. Thermal behavior of fractionated and unfractionated bovine brain cerebrosides. *Biochemistry.* 21:1761–1764.

Curatolo, W., D. M. Small, and G. G. Shipley. 1977. Phase behavior and structural characteristics of hydrated bovine brain gangliosides. *Biochim. Biophys. Acta.* 468:11–20.

Exton, J. H. 1994. Messenger molecules derived from membrane lipids. *Curr. Opinion Cell Biol.* 6:226–229.

Fishman, P. H., T. Pacuszka, and P. A. Orlandi. 1993. Gangliosides as receptors for bacterial enterotoxins. *Adv. Lipid Res.* 25:165–187.

Haas, N. S., and G. G. Shipley. 1995. Structure and properties of *N*-palmitoleoyl-galactosyl-sphingosine (cerebroside). *Biochim. Biophys. Acta.* 1240:133–141.

Hakomori, S., and Y. Igarashi. 1995. Functional role of glycosphingolipids in cell recognition and signaling. *J. Biochem.* 118:1091–1103.

Hannun, Y. A. 1994. Sphingomyelin cycle and the second messenger function of ceramide. *J. Biol. Chem.* 269:3125–3128.

Harouse, J. M., S. Bhat, S. L. Spitalnik, M. Laughlin, K. Stefano, D. H. Silberberg, and F. Gonzalez-Scarano. 1991. Inhibition of entry of HIV-1 in neural cell lines by antibodies against galactosyl ceramide. *Science.* 253:320–323.

Hinz, H.-J., H. Kuttenreich, R. Meyer, M. Renner, R. Frund, R. Koynova, A. I. Boyanov, and B. G. Tenchov. 1991. Stereochemistry and size of sugar headgroups determine structure and phase behaviour of glycolipid membranes: densitometric, calorimetric and x-ray studies. *Biochemistry.* 30:5125–5138.

Mannock, D. A., R. N. McElhaney, P. E. Harper, and S. M. Gruner. 1994. Differential scanning calorimetry and x-ray diffraction studies of the thermoreomeric di-tetradecyl-β-D-galactosyl glycerols and their mixture. *Biophys. J.* 66:734–740.

Nishizuka, Y. 1992. Intracellular signaling by hydrolysis of phospholipids and activation of protein kinase C. *Science.* 258:607–614.

Reed, R. A., J. Mattai, and G. G. Shipley. 1987. Interaction of cholera toxin with ganglioside G$_{M1}$ receptors in supported lipid monolayers. *Biochemistry.* 26:824–832.

Reed, R. A., and G. G. Shipley. 1987. Structure and metastability of *N*-lignoceryl-galactosylsphingosine (cerebroside) bilayers. *Biochim. Biophys. Acta.* 896:153–164.

Reed, R. A., and G. G. Shipley. 1989. Effect of chain unsaturation on the structure and thermotropic properties of galactocerebrosides. *Biophys. J.* 55:281–292.

Reed, R. A., and G. G. Shipley. 1996. Properties of ganglioside G$_{M1}$ in phosphatidylcholine bilayer membranes. *Biophys. J.* 70:1363–1372.

Ruocco, M. J., D. Atkinson, D. M. Small, R. P. Skarjune, E. Oldfield, and G. G. Shipley. 1981. X-ray diffraction and calorimetric study of anhydrous and hydrated *N*-palmitoylgalactosylsphingosine (cerebroside). *Biochemistry.* 20:5957–5966.

Ruocco, M. J., and G. G. Shipley. 1986. Thermal and structural behavior of natural cerebroside 3-sulfate in bilayer membranes. *Biochim. Biophys. Acta.* 859:246–256.

Saxena, K., R. I. Duclos, P. Zimmermann, R. R. Schmidt, and G. G. Shipley. 1999. Structure and properties of totally synthetic galacto- and gluco-cerebrosides. *J. Lipid Res.* 40:839–849.

Schmidt, R. R., and P. Zimmermann. 1986. Synthesis of glycosphingolipids and psychosines. *Angew. Chem. Int. Ed. Engl.* 25:725–726.

Sen, A., S.-W. Hui, D. A. Mannock, R. N. A. H. Lewis, and R. N. McElhaney. 1990. Physical properties of glycosyldiacylglycerols. 2.

X-ray diffraction studies of a homologous series of 1,2-di-*O*-acyl-3-*O*-(α-D-glucopyranosyl)-sn-glycerols. *Biochemistry.* 29:7799–7804.

Sen, A., W. P. Williams, and P. J. Quinn. 1981. The structure and thermotropic properties of pure 1,2-diacylgalactosylglycerols in aqueous systems. *Biochim. Biophys. Acta.* 663:380–389.

Shah, J., J. M. Atienza, R. I. Duclos, Jr., A. V. Rawlings, Z. Dong, and G. G. Shipley. 1995. Physical properties of ceramides: effect of fatty acid hydroxylation. *J. Lipid Res.* 36:1936–1944.

Shipley, G. G., J. P. Green, and B. W. Nichols. 1973. The phase behavior of monogalactosyl, digalactosyl and sulphoquinovosyl diglycerides. *Biochim. Biophys. Acta.* 311:531–544.

van den Berg, L. H., S. A. Sadiq, S. Lederman, and N. Latov. 1992. The gp120 glycoprotein of HIV-1 binds to sulfatide and to the myelin associated glycoprotein. *J. Neurosci. Res.* 33:513–518.

Zhang, R., D. L. Scott, M. L. Westbrook, S. Nance, B. D. Spangler, G. G. Shipley, and E. M. Westbrook. 1995a. The three-dimensional crystal structure of cholera toxin. *J. Mol. Biol.* 251:563–573.

Zhang, R., M. L. Westbrook, E. M. Westbrook, D. L. Scott, Z. Otwinowski, P. R. Maulik, R. A. Reed, and G. G. Shipley. 1995b. The 2.4Å crystal structure of cholera toxin B subunit pentamer: choleragenoid. *J. Mol. Biol.* 251:550–562.

Zimmermann, P., R. Bommer, T. Bar, and R. R. Schmidt. 1988. Azidosphingosine glycosylation in glycosphingolipid synthesis. *J. Carbohydr. Chem.* 7:435–452.